ARTICLE NO. 79-0892R

A80-054

Impact of Far-Aft Center of Gravity for a Single-Stage-to-Orbit Vehicle

40009
40010
60009

Delma C. Freeman Jr.* and Richard W. Powell†
NASA Langley Research Center, Hampton, Va.

Aft center-of-gravity locations dictated by the large number of rocket engines required has been a continuing problem of single-stage-to-orbit vehicle design. Recent work has demonstrated that these aft center-of-gravity problems become more pronounced for the proposed heavy-lift mission, creating some unique design problems for both the single-stage-to-orbit and staged vehicle systems. During this study, an effort was made to bring together automated vehicle design, wind-tunnel tests, and flight control analyses to assess the impact of longitudinal and lateral-directional instability, and control philosophy on entry vehicle design technology.

Nomenclature

b = reference span, m

C_l = rolling-moment coefficient = $\dfrac{\text{rolling moment}}{q_\infty Sb}$

C_{l_β} = $\partial C_l/\partial\beta$, rad^{-1} or deg^{-1}

C_m = pitching-moment coefficient = $\dfrac{\text{pitching moment}}{q_\infty S\bar{c}}$

C_N = normal-force coefficient = $\dfrac{\text{normal force}}{q_\infty S}$

C_n = yawing-moment coefficient = $\dfrac{\text{yawing moment}}{q_\infty Sb}$

C_{n_β} = $\partial C_n/\partial\beta$, rad^{-1} or deg^{-1}

$C_{n_{\beta_{dyn}}}$ = $C_{n_\beta}\cos\alpha - (I_Z/I_X)C_{l_\beta}\sin\alpha$

$\bar{c}$ = mean aerodynamic chord, m

I_X, I_Y, I_Z = moment of inertia about X, Y, and Z body axes, kg m^2

I_{XZ} = product of inertia, kg m^2

l = model body length (nose-to-body-flap hingeline), m

M = Mach number

q_∞ = freestream dynamic pressure, Pa

S = reference area, m^2

X, Y, Z = body reference axes

α = angle of attack, deg

β = angle of sideslip, deg

δ_{BF} = body-flap deflection, positive when trailing edge is down, deg

δ_E = elevon deflection, positive when trailing edge is down, deg

δ_R = rudder deflection, positive trailing edge left, deg

δ_{SF} = side-force generator deflection, positive trailing edge right, deg

δ_{TF} = tip fin control deflection, positive right controller deflected outboard, deg

ΔC_l = rolling moment due to yaw control = $(C_{l_{\delta_{TF=-40}}} - C_{l_{\delta_{TF=0}}})$

ΔC_n = yaw control effectiveness = $(C_{n_{\delta_{TF=-40}}} - C_{n_{\delta_{TF=0}}})$

Introduction

BECAUSE of their relative simplicity, single-stage-to-orbit (SSTO) vehicle systems are attractive candidates for future Earth-orbital transportation systems. The aft center-of-gravity (c.g.) location caused by the large engine mass at the rear of the vehicle creates significant stability and control problems for SSTO designs. Currently, advanced systems studies project the need for two classes of vehicle systems, a priority vehicle and a heavy-lift vehicle. The priority vehicle would be developed primarily for applications requiring a quick response capability to deliver a 10- to 50-metric-ton payload to orbit. The heavy-lift vehicle would be required to support development of large structures in space and would have a 200- to 1000-metric-ton payload capability.

The vehicle design used in the present study has evolved from the work presented in Refs. 1 and 2. For the study, a Mach $-\alpha$ profile was tailored to the longitudinal trim capability of the vehicle with the primary design consideration being the ability to achieve longitudinal trim in the Mach 3-5 regime. Once the entry profile was established, all subsequent entries were made using this profile (presented in Fig. 1). Different entry profile shapes could change the lateral-directional control requirements, but since longitudinal trim requirements are the limiting factor, different entry profiles would not affect the results of this study, except where noted.

The results of systems studies are presented in Fig. 2 where the projected c.g. ranges are shown for both priority and heavy-lift vehicles during entry. These results show projected c.g. ranges from 0.71 to 0.74 body length for the priority vehicle and from 0.76 to 0.78 body length for the heavy-lift

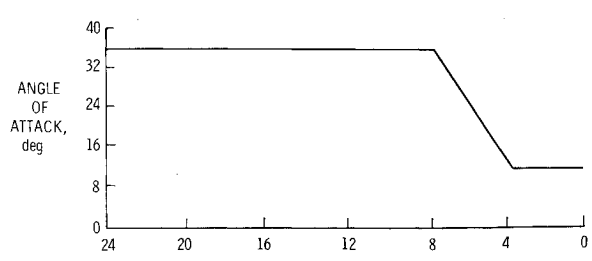

Fig. 1 Mach $-\alpha$ entry profile.

Presented as Paper 79-0892 at the AIAA/NASA Conference on Advanced Technology for Future Space Systems, Hampton, Va., May 8-11, 1979; submitted June 18, 1979; revision received Feb. 28, 1980. This paper is declared a work of the U.S. Government and therefore is in the public domain.

Index categories: LV/M Propulsion and Propellant Systems; LV/M Mission Studies and Economics; Liquid Rocket Engines and Missile Systems.

*Aerospace Engineer, Space Systems Division. Member AIAA.
†Aerospace Engineer, Space Systems Division.

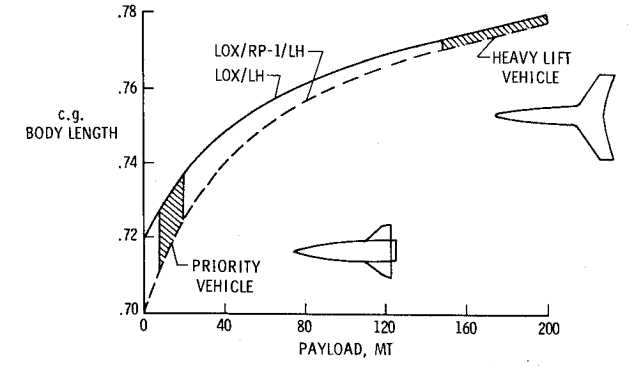

Fig. 2 Center-of-gravity characteristics for winged SSTO's during entry.

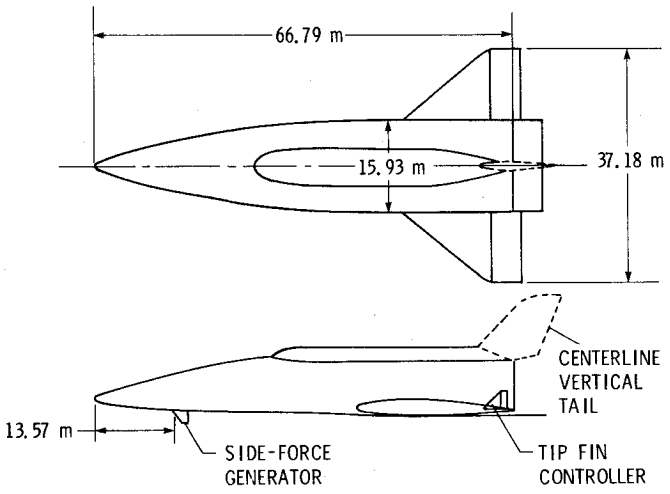

Fig. 3 Drawing showing study configuration with modifications.

vehicles. These locations compare to a c.g. range of 0.65-0.67 body length for the Space Shuttle Orbiter during entry. The c.g. is further aft in SSTO vehicles than in the Space Shuttle because of increased propulsion system mass that results from no staging and a difference in vehicle density because the SSTO is essentially a large fuel tank. With these aft c.g. locations projected for the advanced vehicle systems, unique stability and control problems exist.

There has been a continuing program over the past several years to study the impact of relaxing the longitudinal and lateral-directional stability requirements of SSTO vehicle designs. From this work, a study vehicle has been developed; aerodynamic, mass properties, and systems design information has been generated to provide sufficient data to simulate six-degree-of-freedom (6-DOF) entries with the Program to Optimize Simulated Trajectories (POST).[3] A drawing of the configuration, as it has evolved, is presented in Fig. 3. The geometric characteristics and mass properties of the study vehicle are presented in Tables 1 and 2.

The approach that has been taken in analyzing the aft c.g. location problem has been to utilize the study configuration and its aerodynamics and mass properties data base for 6-DOF POST entry simulations. Entries with a range of c.g. locations from 0.68 to 0.73 (longitudinal trim range) body length have been run, and analyses have been made of both the longitudinal and lateral-directional stability levels encountered. Ways have also been investigated to augment the available lateral-directional control and to extend the c.g. range which is limited by the longitudinal trim requirements. Trade studies have been made to assess these configuration/control system modifications in terms of total reaction control system (RCS) firing time used during entry.

Table 1 Geometric characteristics of the study vehicle

Length, m	55.63
Wing span, m	37.63
Leading edge wing sweep, deg	50
Reference wing area, m^2	577.1
Exposed wing area, m^2	227.7
Elevon area, m^2	89.49
Wing section	
Tip	0010-64[a]
Root	0008-64[a]

[a] From Ref. 4.

Table 2 Mass properties of the study vehicle

Gross liftoff weight, kg	1.5×10^6
Entry weight, kg	1.9×10^6
Payload, kg	2.9×10^4
Study c.g. range	0.68-0.73l
I_X, kg m^2	7.53×10^5
I_Y, kg m^2	1.15×10^8
I_Z, kg m^2	6.60×10^7
I_{XZ}, kg m^2	7.54×10^5

Table 3 RCS jet characteristics

Pitch, N·m	9.6×10^4
Yaw, N·m	4.0×10^5
Roll, N·m	3.3×10^5

The control system modeled for the study was similar to that of the space shuttle, utilizing a mixture of RCS and aerodynamic controls to fly the desired entry trajectory. The control scheme used for the SSTO was different in that its RCS was used from entry to landing. The moments generated by the RCS are given in Table 3.

Conventional elevons were used for both pitch and roll control.

Longitudinal and Lateral-Directional Stability

In order to assess the impact of the large instabilities resulting from the far-aft c.g. locations projected for future space transportation systems, a series of entry simulations were made at various c.g. locations. The most aft c.g. location flown was 0.73 body length because this was the limiting case for longitudinal trim. The longitudinal and lateral-directional stability levels flown in the simulation with the c.g. at 0.73 body length are presented in Fig. 4. The longitudinal stability level is shown in terms of static margin and $C_{n_{\beta_{dyn}}}$ as functions of entry Mach number. Also presented for comparison with the current technology entry vehicle system are the predicted stability levels of the space shuttle at its most aft operational c.g. location of 0.675 body length. The results show that in the hypersonic speed regime the study vehicle is slightly unstable down to a Mach number of 5.0. Below Mach 5.0, because of a forward shift in the aerodynamic center, the vehicle becomes quite unstable; at a Mach number of 3.0, the vehicle is 0.30 $\bar{c}$ unstable. This level of instability corresponds to a time-to-double amplitude of 0.72 s. Decreasing the Mach number below 3.0 results in a decrease in the level of instability as the aerodynamic center shifts aft and transonic Mach numbers are approached. At 0.6 Mach number, there is a large instability that is the result of a pitchup which could be eliminated with some detailed configuration work in this speed regime. The comparison with the space shuttle shows that nowhere during entry is the shuttle nearly as unstable as the study vehicle.

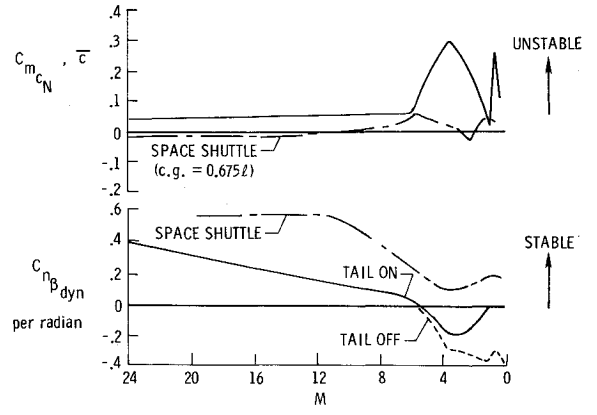

Fig. 4 Longitudinal and lateral-directional stability characteristics ove entry Mach range for c.g. at 0.73*l*.

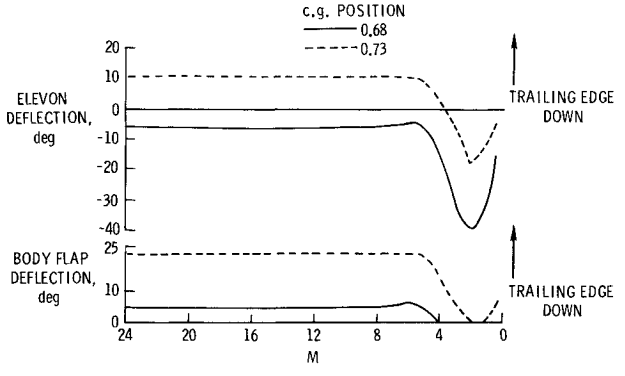

Fig. 5 Effect of c.g. position on longitudinal trim.

Also presented on Fig. 4 is a comparison of the lateral-directional stability parameter $C_{n_{\beta_{dyn}}}$ for the study configuration and the space shuttle. These results show that in the hypersonic speed regime the study configuration had a positive value of $C_{n_{\beta_{dyn}}}$; at Mach numbers below 5.0, $C_{n_{\beta_{dyn}}}$ becomes negative for both the vertical tail-on and -off configurations. For the Space Shuttle, $C_{n_{\beta_{dyn}}}$ is positive throughout the entry.

Longitudinal Trim

The results of entry simulations to determine the trimmable c.g. range are presented in Fig. 5. The elevon and body-flap deflections required to trim the vehicle are presented for the most forward (0.68*l*) and the most aft (0.73*l*) c.g. positions flown in the simulations over the entry Mach number range. For the 0.68*l* c.g. position in the hypersonic speed regime, only small body-flap and elevon deflections are required to trim the vehicle. At a Mach number of approximately 5.0, the negative elevon deflection required to trim became larger; at transonic Mach numbers, almost all of the allowable deflection is required for trim. For an entry with a c.g. position of 0.675*l*, the vehicle could not be trimmed in the transonic speed regime, and it diverged. At the aft c.g. location (0.73*l*) in th hypersonic speed regime, maximum body-flap deflection is required in addition to a 10-deg positive elevon deflection. In the supersonic speed range, both the body-flap and elevon deflections required for trim are reduced; at transonic and subsonic Mach numbers, negative elevon deflections are required for trim. For an entry with the c.g. located at 0.735*l*, the downward elevon deflection required to trim the vehicle in the hypersonic speed regime became so large that all of the allowable deflection was required for trim, and the vehicle diverged because of loss of roll control.

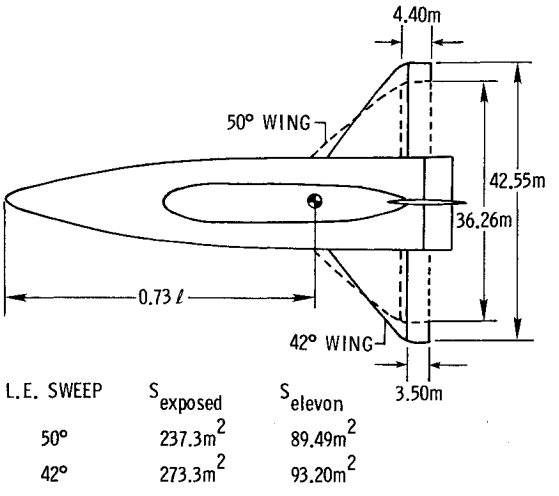

Fig. 6 Comparison of 42- and 50-deg wings.

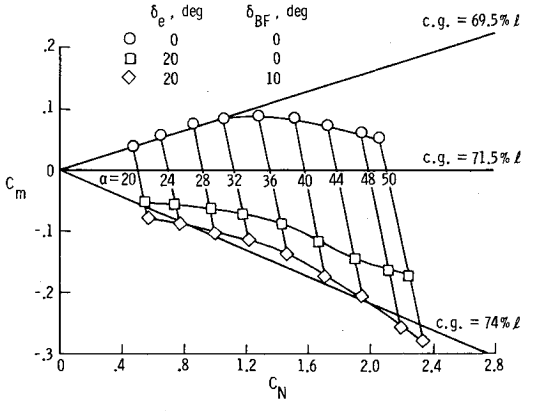

Fig. 7 Hypersonic trim characteristics of 42-deg swept wing at *M*=20.3.

One approach that was taken in the study to extend the flyable c.g. range further aft for the study vehicle was to reduce the wing leading-edge sweep. The best estimates available indicated that leading-edge wing sweeps of less than 40 deg would create difficult heating problems. Based on these estimates, a 42-deg swept wing was designed for the study configuration with approximately the same total reference area, but having considerably more exposed area aft of the vehicle c.g. (see Fig. 6). The hypersonic trim capability of the study vehicle with the reduced wing sweep was examined at Mach 20.3 in the NASA Langley Research Center hypersonic helium tunnel facility, and the results are presented in Fig. 7.[5] These results show that with the combination of maximum elevon and body-flap deflection, the vehicle can be trimmed at a c.g. location of 0.74*l*. Decreasing the wing sweep from 50 to 42 deg resulted in about a 1% aft shift in the allowable c.g. range. Analyses are now in progress to determine the effects of the 42-deg swept wing on the vehicle flight control characteristics and c.g. location.

RCS Fuel Usage Trade Studies

Throughout the aft c.g. studies, several trade studies were made to assess the impact of various configuration parameters on the amount of RCS fuel required for entry. The results of some of these studies are presented in Table 4. The total RCS jet firing time is presented in the table as a function of configuration changes such as vertical tail-off and -on, lateral c.g. offset, and longitudinal c.g. position. The first trade study was to determine the impact of c.g. position on the entry RCS fuel usage. Entries were made at the most forward (0.68*l*) and most aft (0.73*l*) c.g. positions. The results

Table 4 Effect of study variables on RCS fuel usage—6-DOF POST entry simulations

Longitudinal c.g. position	Latitude c.g. offset, m (in.)	Vertical tail	Total RCS on time, s
68	0	on	153
73	0	on	120
73	0	off	144
73	0.101(4)	on	160
73	0.101(4)	off	192

of these entries were not as expected since there was very little difference in the amount of RCS jet firing times at the two c.g. locations. However, a closer look at the aerodynamics of the configuration shows that because of the large surfaces and trim deflections, the hypersonic trimmed L/D is reduced from 1.5 at the aft c.g. location (0.73l) to 1.25 at the forward c.g. location (0.68l). This large difference in the aerodynamic performance results in a significant difference in the vehicle planform loading and, therefore, impacts the required maneuvers to stay within heating constraints and to achieve the desired crossrange. In order to properly assess this trade, optimum trajectories are being generated for both the forward and aft c.g. locations.

The second trade study was to determine the effect of removing the centerline vertical tail. Systems design studies have estimated the weight savings for removing the vertical tail at between 3,600 and 4,500 kg, which translates to a 0.01l forward shift in the c.g. position. Because of these projected benefits, attempts have been made to devise a control scheme that will enable the vehicle to fly with the center vertical tail removed. Presented in Table 4 are the results of a trade study to determine the impact of removing the vertical tail on the entry RCS fuel usage. The comparison shows very little increase in the amount of RCS fuel used when the vertical tail is removed. This can be explained since, as shown in Fig. 4 with the far-aft c.g. location, the vehicle is directionally unstable even with the vertical tail-on. The major problem that arises from removal of the center vertical tail is the loss of a rudder for use in trimming out vehicle asymmetries and lateral c.g. offsets. This point is demonstrated in the last of the RCS fuel trade studies presented in Table 4 where a 10-cm lateral c.g. offset results in a significant increase in RCS fuel required for entry.

Tip Fin Controller

In an attempt to decrease the RCS fuel used for the lateral c.g. offset and to increase the amount of available yaw control, tip fin controllers were installed on the study configuration. A sketch of the model with the tip fin controller is presented in Fig. 3, and a sketch of the tip fin is presented in Fig. 8. The fins were sized [approximately 8.64 m^2 (93 ft^2) per side] to accommodate the yaw and roll RCS jets to take advantage of increased moment arm and to minimize the jet interference with the aerodynamic surfaces. Yaw control is obtained by outward deflection of the outboard surface of a single fin. Both outboard surfaces are deflected symmetrically outward for speedbrake applications. Wind-tunnel tests were conducted to determine the control effectiveness of the tip fin controller, and selected results are presented in Fig. 9. Comparisons are shown for yaw (ΔC_n) and roll (ΔC_l) due to tip fin deflection as a function of Mach number as well as the rudder effectiveness for the space shuttle with a deflection of 10 deg. These results show that deflecting the tip fin controller 20 deg produced about the same yaw control in the supersonic speed regime as the space shuttle rudder deflected 10 deg (maximum shuttle rudder deflection is 22.8 deg). Deflecting the tip fin controller 40 deg made the control surface quite effective in the Mach number range from 2.36-4.63. At transonic and subsonic Mach numbers, the tip fin controller

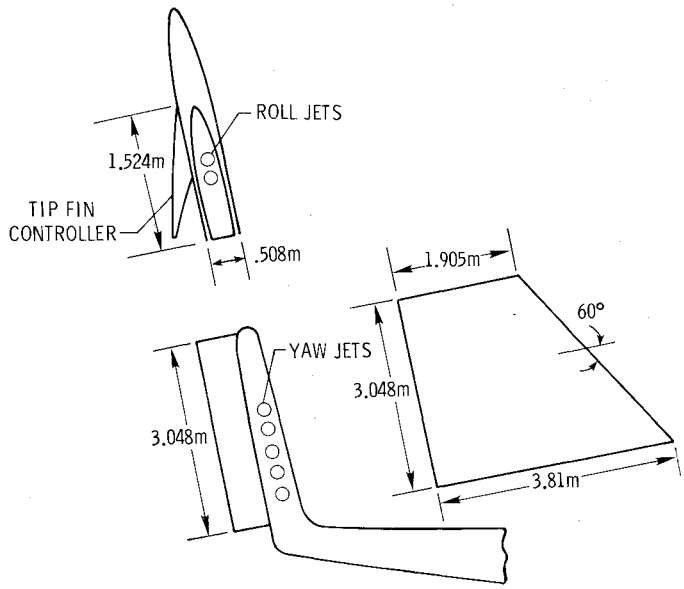

Fig. 8 Sketch of tip fin controller.

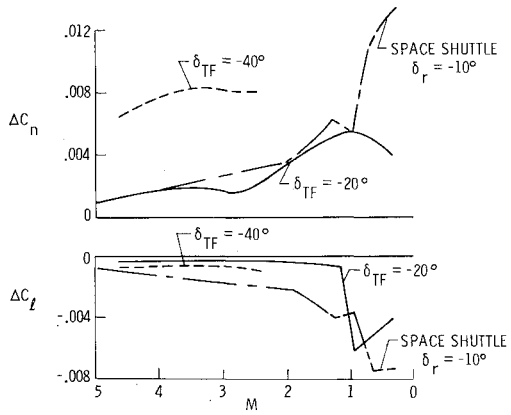

Fig. 9 Tip fin controller effectiveness.

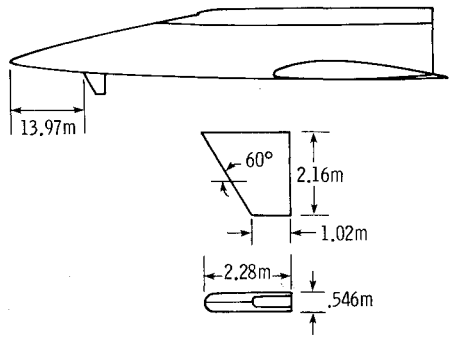

Fig. 10 Sketch of side-force generator.

was not as effective as the space shuttle rudder. The rolling moment due to deflection of the tip fin controller was very small in the supersonic speed regime, indicating that the tip fin controller is a pure yaw device.

Side-Force Generator

In an attempt to provide the yaw control necessary to satisfy crosswind landing requirements, a deployable side-force generator was installed on the model, as shown in Fig. 10. This side-force generator was envisioned as a device that would be deployed with the landing gear during the final approach and landing phases of entry flight. Subsonic wind-

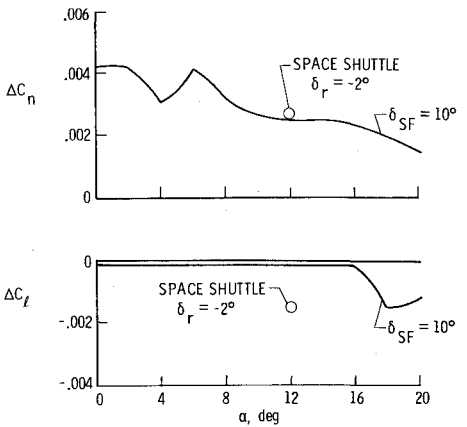

Fig. 11 Side-force generator control effectiveness at $M = 0.3$.

tunnel tests were conducted to determine the control effectiveness of the side-force generator, and the results are presented in Fig. 11. The results show that at landing attitude ($\alpha = 12$ deg) the side-force generator with 10-deg deflection has the same effectiveness as the rudder with 2-deg deflection. Based on these data, the side-force generator, as designed, does not provide sufficient yaw control to meet crosswind landing requirements.

Conclusions

The overriding design consideration dictated by the aft center-of-gravity locations projected for future single-stage-to-orbit space transportation systems is that control configuring is a requirement, not an option.

The 6-DOF of entry simulations have shown that the major design problems associated with the far-aft center-of-gravity locations are the need for methods to obtain additional longitudinal trim capability and the use of new approaches for lateral-directional control.

System design studies have shown that removing the centerline vertical tail moves the vehicle center of gravity forward approximately 0.01 body length. Tip fin controllers in combination with an RCS appear to give sufficient yaw control and trim to possibly allow removal of the vertical tail.

Because of the unique nature of the aft center-of-gravity problem, there is a requirement that aerodynamic, aeroheating, flight control, and system design studies be closely integrated.

References

[1] Hepler, A.K., Zeck, H., Walker, W.H., and Shafer, D.E., "Applicability of the Control Configured Design Approach to Advanced Earth-Orbital Transportation System," NASA CR-2723, Aug. 1978.

[2] Freeman, D.C., Jr. and Wilhite, A.W., "Effects of Relaxed Static Longitudinal Stability on a Single-Stage-to-Orbit Vehicle Design," NASA TP-1594, 1979.

[3] Brauer, G.L., Cornick, D.E., and Stevenson, R., "Capabilities and Applications of the Program to Optimize Simulated Trajectories (POST)," NASA CR-2770, Feb. 1977.

[4] Abbott, I.H. and VanDoenhoff, A.E., *Theory of Wing Sections,* Dover Publications, New York, 1959.

[5] Bernot, P.T., "Aerodynamic Characteristics of Two Single-Stage-to-Orbit Vehicles at Mach 20.3," NASA TM X-3550, 1977.